A Numerical Scheme for the Boltzmann Equation

Hans Babovsky

Institute of Mathematics, Ilmenau Technical University, Weimarer Str. 25, D-98693 Ilmenau, Germany

Abstract. We present a numerical scheme for the Boltzmann equation which is based on a regular hexagonal lattice of velocity space. As shown in previous work, such discretizations satisfy all theoretical requirements of kinetic theory. Here, we demonstrate its practical versatility. In particular, we demonstrate its applicability for flow simulations in various fluid dynamic limits.

All results presented here concern the 2D velocity space. 3D results are in progress.

Keywords: Boltzmann equation, numerical scheme, fluid dynamic limits
PACS: 47.45.-n, 02.60.-x, 47.40.-x

INTRODUCTION

The classical numerical tool for the simulation of the Boltzmann equation are Monte Carlo schemes. These have proven to be a reliable algorithm in a number of real applications. However, as a stochastic method, they suffer from fluctuations. Thus some situations are hard to be resolved by these, for example small perturbations of Maxwellians close to the fluid dynamic limit; in addition, small Knudsen numbers turn out to be very expensive.

In [1], a discretization of the Boltzmann collision operator has been proposed which since then has turned out to be particularly useful for numerical simulations in the transition regime (see [2, 3]). In the present paper, we discuss a slight modification. It results in a simplified discretization of a 2D velocity space and is given by a regular lattice. As the main objective of this paper, we demonstrate that this algorithm is applicable for small perturbations as well as very small Knudsen numbers and that it is therefore a useful tool to study various fluid dynamic limits of the Boltzmann equation.

For our numerical examples, we take up the work of F. Golse and others (see [4] and the papers cited there). They have investigated different scaling limits for the Boltzmann equation starting from small perturbations of a global Maxwellian. Their results cover the compressible and incompressible Euler and Navier Stokes equations limits. We present numerical results illustrating these. Our algorithm is applicable for very small Knudsen numbers and thus reaches close to the fluid dynamic limits.

THE BOLTZMANN EQUATION

The homogeneous version

The space homogeneous Boltzmann equation

$$\partial_t f = J[f,f] \tag{1}$$

in d-dimensional velocity space ($d = 2,3$) is an evolution equation for a density $f = f(t,\mathbf{v})$ in $\mathbb{R}^d$ with the collision operator $J[f,f]$ having the form

$$J[f,f](\mathbf{v}) = \int_{\mathbf{w}\in\mathbb{R}^d}\int_{S^{d-1}} \tilde{k}(|\mathbf{v}-\mathbf{w}|,\alpha)[f(\mathbf{v}')f(\mathbf{w}') - f(\mathbf{v})f(\mathbf{w})]d\zeta d\mathbf{w} \tag{2}$$

Here, $\tilde{k}$ is a nonnegative integral kernel, S^{d-1} is the surface of the unit sphere in $\mathbb{R}^d$, α is the angle between $\mathbf{v}-\mathbf{w}$ and $\zeta \in S^{d-1}$, and $\mathbf{v}'$ and $\mathbf{w}'$ are given as

$$\mathbf{v}' = \frac{\mathbf{v}+\mathbf{w}}{2} + \frac{1}{2}|\mathbf{v}-\mathbf{w}|\zeta, \quad \mathbf{w}' = \frac{\mathbf{v}+\mathbf{w}}{2} - \frac{1}{2}|\mathbf{v}-\mathbf{w}|\zeta. \tag{3}$$

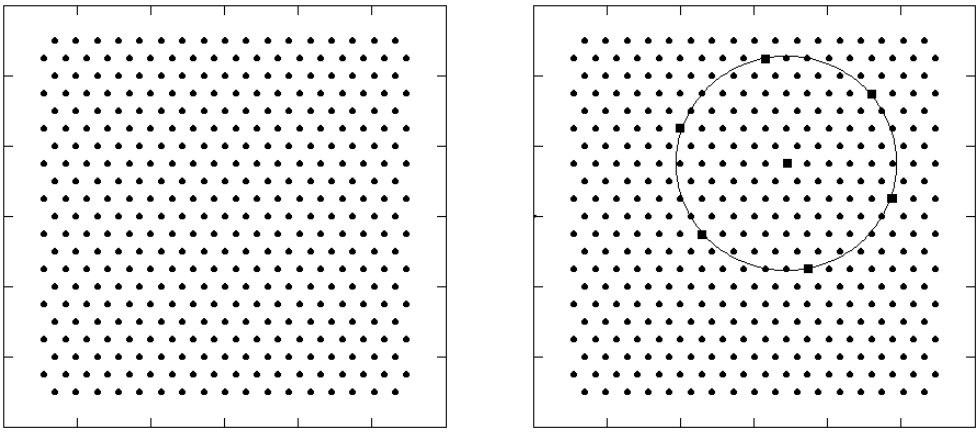

FIGURE 1. (a) The grid $\mathscr{C}_h$. (b) Regular hexagon on circle.

For given $\mathbf{v},\mathbf{w} \in \mathbb{R}^d$, we define the center $\mathbf{c}$ and the polar coordinates of the difference $\mathbf{v}-\mathbf{c}$,

$$\mathbf{c} = \mathbf{c}(\mathbf{v},\mathbf{w}) := \frac{\mathbf{v}+\mathbf{w}}{2} \quad \text{and} \quad r\cdot\omega := \mathbf{v}-\mathbf{c} \quad \text{with} \quad r \geq 0, \quad \omega \in S^{d-1}. \tag{4}$$

This leads to the formulas

$$\mathbf{v} = \mathbf{c}+r\cdot\omega, \quad \mathbf{w} = \mathbf{c}-r\cdot\omega, \quad \mathbf{v}' = \mathbf{c}+r\cdot\zeta, \quad \mathbf{w}' = \mathbf{c}-r\cdot\zeta; \tag{5}$$

writing $k(.,.) := 2^d\tilde{k}(.,.)$, the collision operator reads

$$J[f,f](\mathbf{v}) = \int_{\mathbf{c}\in\mathbb{R}^d}\int_{S^{d-1}} k(2r,\alpha)[f(\mathbf{c}+r\cdot\zeta)f(\mathbf{c}-r\cdot\zeta) - f(\mathbf{c}+r\cdot\omega)f(\mathbf{c}-r\cdot\omega)]d\zeta d\mathbf{c} \tag{6}$$

In addition, a weak formulation can be derived by multiplying with a test function $\phi(\mathbf{v})$ and integrating. Applying the well-known transformation formulas we end up with

$$\partial_t\langle\phi,f\rangle = \int_{\mathbb{R}^d}\int_{\mathbb{R}^d}\int_{S^{d-1}} k(2r,\alpha)[\phi(\mathbf{c}+r\zeta)-\phi(\mathbf{c}+r\omega)]f(\mathbf{c}+r\omega)f(\mathbf{c}-r\omega)d\zeta d\mathbf{v}d\mathbf{c} \tag{7}$$

where we have used the abbreviation

$$\langle\phi,f\rangle = \int_{\mathbb{R}^d}\phi(\mathbf{v})f(\mathbf{v})d\mathbf{v} \tag{8}$$

The discretized collision operator

Fur numerical purposes, the integral $\int_{\mathbb{R}^d}\int_{\mathbb{R}^d}\int_{S^{d-1}} d\zeta d\mathbf{v}d\mathbf{c}$ of (7) has to be replaced by a sum. Here, we consider only the case $d=2$. (For the three-dimensional case, see Remark (b) below.) For the discretization of the four-dimensional *outer* integral $d\mathbf{v}d\mathbf{c}$, we identify $\mathbb{R}^2$ with the complex plane $\mathbb{C}$. Given a (small) parameter $h>0$, $\mathbb{C}$ is discretized by the regular lattice

$$\mathscr{C}_h = h\cdot\{k+\ell\cdot\exp(2\pi i/6) : k,\ell\in\mathbf{Z}\}, \tag{9}$$

and the integral $\int_{\mathbb{R}^2}\int_{\mathbb{R}^2} d\mathbf{v}d\mathbf{c}$ is replaced by the sum $\sum_{\mathbf{v},\mathbf{c}\in\mathscr{C}_h}$. The crucial observation for the discretization of the *inner* integral $d\zeta$ is that for any $\mathbf{c}\in\mathscr{C}_h$, $\mathscr{C}_h = \mathbf{c}+\exp(2\pi i/6)\cdot\mathscr{C}_h$, i.e. $\mathscr{C}_h$ has translational and hexagonal rotational symmetry. As a consequence, given any $\mathbf{c},\mathbf{v}\in\mathscr{C}_h$, the regular hexagon around $\mathbf{c}$ containing $\mathbf{v}$ lies on $\mathscr{C}_h$. More precisely, with $\mathbf{z}_0 := \mathbf{v}-\mathbf{c}$, all nodes of the hexagon $(\mathbf{v}_k, k=0,\ldots,5)$ defined by $\mathbf{v}_k = \mathbf{c}+\mathbf{z}_0\cdot\exp(2\pi ik/6)$ lie in $\mathscr{C}_h$. Fig. 1 illustrates this. Thus it is near at hand to replace the collision integral

$$\int_{S^1} k(2r,\alpha)[f(\mathbf{c}+r\cdot\zeta)f(\mathbf{c}-r\cdot\zeta) - f(\mathbf{c}+r\cdot\omega)f(\mathbf{c}-r\cdot\omega)]d\zeta \tag{10}$$

FIGURE 2. (a) Propagation of shock into channel (a) early stage (b) later stage

by the sum

$$\bar{k}(2r)\cdot\frac{1}{3}\sum_{\ell=0}^{2}[f(\mathbf{v}_\ell)f(\mathbf{v}_{\ell+e})-f(\mathbf{v}_0)f(\mathbf{v}_3)]\quad\text{with (e.g.)}\quad\bar{k}(2r)=(2\pi)^{-1}\int_0^{2\pi}k(2r,\alpha)d\alpha. \tag{11}$$

A complete kinetic theory on hexagonal grids has been derived in [1], where it has been shown, that the discrete Boltzmann equation meets all the requirements of the continuous one (conserved quantities, H theorem, linearized operator etc.). Furthermore, the lattice satisfies the imbedding property $\mathscr{C}_h\subset\mathscr{C}_{h/2}$. As was shown in [2], the continuum limit $h=2^{-N}$ with $N\to\infty$ results in a Boltzmann equation on $\mathbb{R}^2$ of the form

$$\partial_t f(\mathbf{v})=\int_{\mathbf{c}\in\mathbb{R}^2}\int_{S^1}\hat{k}(2|\mathbf{v}-\mathbf{c}|)[f(\mathbf{c}+r\cdot\zeta)f(\mathbf{c}-r\cdot\zeta)-f(\mathbf{c}+r\cdot\omega)f(\mathbf{c}-r\cdot\omega)]d\zeta_6(\mathbf{c},\mathbf{v})d\mathbf{c} \tag{12}$$

where $\int_{S^1}d\zeta_6(\mathbf{c},\mathbf{v})$ describes the summation over the hexagon corresponding to $\mathbf{c}$ and $\mathbf{v}$ as indicated in (11).

Remarks: (a) There are several ways to discretize the Boltzmann collision operator on regular grids. In this context we have to mention the paper by Rogier and Schneider [5] for rectangular grids. However, as was proven in [6], the order of consistency is very low. We do not know of any attempts to use this scheme for the simulation of space dependent problems.

(b) The first Boltzmann scheme with hexagonal symmetry was developed for a slightly coarser grid than that described above (see [1]). Define $\mathscr{D}_h\subset\mathscr{C}_h$ by

$$\mathscr{D}_h=\sqrt{3}\cdot\exp(2\pi i/12)\cdot\mathscr{C}_h=\{k+\ell\cdot\exp(2\pi i/6):(k-\ell)\bmod 3\neq 0\}. \tag{13}$$

The Voronoi cells corresponding to $\mathscr{D}_h$ yield a partition of $\mathbb{R}^2$ into regular hexagons; their nodes are given by the set

$$\mathscr{G}_h=\mathscr{C}_h\setminus\mathscr{D}_h. \tag{14}$$

If we discretize the pairs $(\mathbf{v},\mathbf{c})$ in the integral (7) by $\mathscr{G}_h\times\mathscr{C}_h$ rather than by $\mathscr{C}_h\times\mathscr{C}_h$ we end up with the algorithm described in [1]. Since it is based upon a partition of $\mathbb{R}^2$, we call it *strongly coupled* in contrast to alternatively developed *loosely coupled* systems [7] which are useful for the generalization to 3D velocity spaces [8]. The results derived in [1] extend easily to the larger $\mathscr{C}_h\times\mathscr{C}_h$ system.

Numerical experiments in the space dependent case

In the second part of the paper we are going to discuss some numerical experiments for the *space-dependent* Boltzmann equation for $f=f(t,\mathbf{x},\mathbf{v})$,

$$(\partial_t+\mathbf{v}\cdot\nabla_{\mathbf{x}})f=J[f,f]. \tag{15}$$

As position space, we choose some rectangle $\Omega=[x_0,x_1]\times[y_0,y_1]$, with appropriate boundary conditions (inflow/outflow, specular/reverse or diffuse reflection). For the coupling of free flow and collision operator we apply the commonly used operator splitting ansatz. The position space is discretized with regular grids with sizes

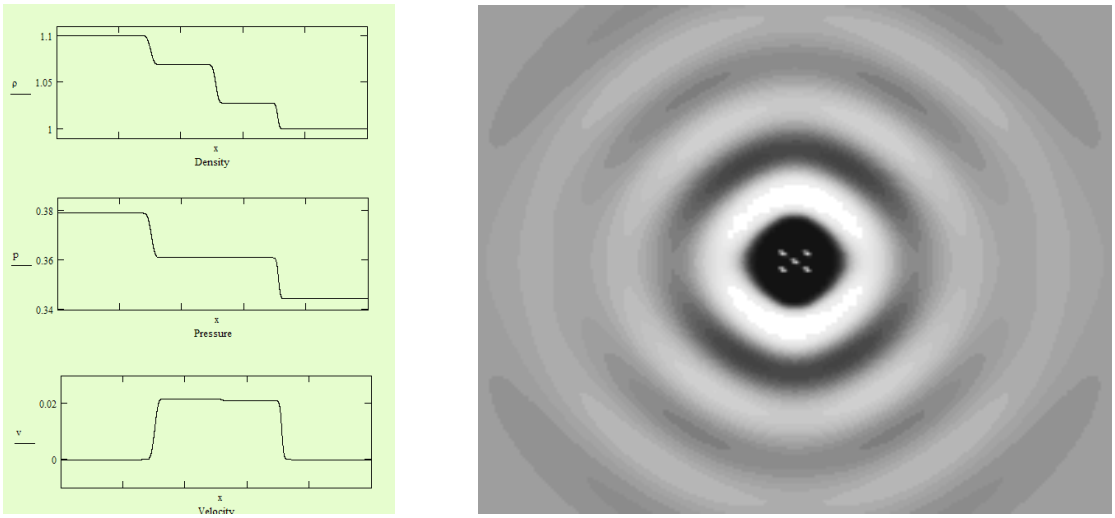

FIGURE 3. Euler limits. (a) Shock tube problem, (b) acoustic wave.

between 45×42 and 300×150 grid points. For the $(\mathbf{v},\mathbf{c})-$discretization we apply the grid $\mathscr{G}_h\times\mathscr{C}_h$ of the above remark which has 2/3 of the size of the original grid $\mathscr{C}_h\times\mathscr{C}_h$. For numerical purposes, both grids $\mathscr{C}_h$ and $\mathscr{G}_h$ are truncated, and we end up with a 133-center points, 96-velocity points system. (As an illustration: the circle in Fig. 1(b) contains 109 center points.) The discretized $(\mathbf{x},\mathbf{v})-$phase space consists of up to $300\times 150\times 96 = 4.32$ Mio. grid points.

In previous papers [2, 3] we have already discussed the applicability of this numerical scheme in the transition regime, e.g. for the calculation of shock fronts showing up in supersonic flows in the presence of walls, or for the calculation of convection driven flows. Most of these numerical experiments were concerned with the calculation of asymptotic steady states. However, since the present algorithm is based on a time marching scheme (in contrast e.g. to the system presented in [9]), we are also able to resolve complex details of the time evolution. We demonstrate this with a simple example.

In Fig. 2, you see find a shock front propagating from the left into a channel with Mach 4.7 and with an angle of attack of 30°. The upper channel wall coincides with the upper line of the picture, the lower wall becomes visible as the flow propagates. We observe the emergence of a shock at the leading edge with a rarefaction zone arising below the lower plate. In the interior of the channel, we recognize a shock front moving into the medium at rest. At a later stage, we find portion of the flow reflected at the upper wall. For the calculation we used a 300×28 spatial grid.

FLUID DYNAMIC LIMITS

Introductory remarks

Classically, the bridge between Boltzmann equation and Fluid Dynamics was established by formal series expansions of solutions of the Boltzmann equation with respect to a small Knudsen number ε. In the Hilbert expansion, the highest order terms lead to the Euler equations while the Navier-Stokes equations appear in the Chapmann-Enskog expansion. This transition has been studied in a more mathematical - yet still formal - framework in [10]. Various types of fluid dynamic limits under different scalings have since then been derived by Golse et al. (see the review paper [4]). The starting point is the rescaled BE

$$\varepsilon^p\partial_t f+\mathbf{v}\cdot\nabla_{\mathbf{x}} f=\varepsilon^{-q}J(f,f) \tag{16}$$

with appropriately chosen powers $p,q\in\mathbb{N}_0$. The work described in [4] is a moment method and concerns slight perturbations of a global Maxwellian. Depending on the powers of ε and the initial data, the resulting equations may be compressible or incompressible Euler or Navier-Stokes systems or variants of these. From

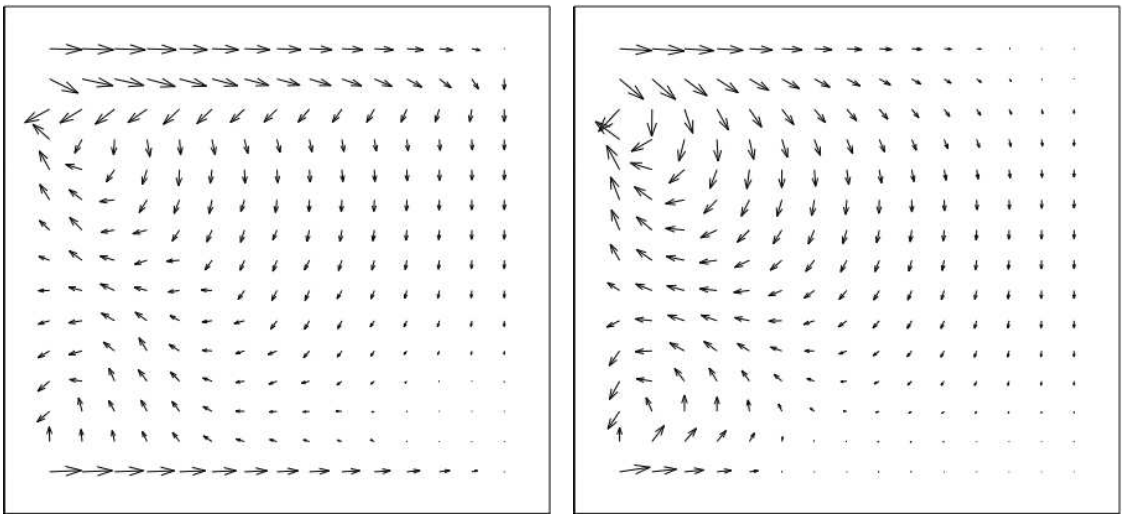

FIGURE 4. (a) Vortices close to the incompressible limit. (a) Moderate, (b) small Knudsen number.

a mathematical point of view, they belong to different types of partial differential equations (in the context of hyperbolic, parabolic, elliptic or mixed types of PDE's). It is our intention to demonstrate that the numerical scheme for the Boltzmann equation presented above is capable of approaching each of these limits.

In a previous paper [3] we have already discussed the shock tube problem as an example for the compressible Euler limit (see the numerical example below). Furthermore, solutions of the Boltzmann equation quite close to the *incompressible Navier-Stokes system* have been numerically calculated in [2], where convection driven flows in a gravitational field with a partially heated lower wall have been obtained. The present paper is concerned with various scaling limits for the Boltzmann equation under small perturbations of a global Maxwellian.

Scaling limits

Euler limits. A characteristic property of the Euler equations as a hyperbolic system is the emergence of shocks. There is no indication in the Boltzmann equation that such shocks may appear in the limit. A typical test problem for numerical schemes in the compressible case is the *shock tube problem*, - a spatially one-dimensional problem where the two halves of a tube are separated by a membrane and contain a gas under different pressures. When the membrane is released, a scenario shows up (in the Euler limit) including a rarefaction zone, a shock front and in between a contact discontinuity. As is shown in Fig. 3(a), these details can be verified in the Boltzmann system, however with viscous effects smearing out the shock front.

The *acoustic system* arises from small perturbations of a global Maxwellian in the Euler scaling (i.e. $p = 0$ and $q = 1$ in formula (16)) and is given by the linearized Euler equations. In our numerical example, we calculated the expansion of a small periodic density perturbation from a source (in the center of the calculational domain) into an infinite channel with reflecting walls. We chose the Knudsen number $\mathrm{Kn} \approx 10^{-3}$ (compared to the height of the channel). The amplitude of the perturbation is 3% of the global density. Fig. 3(b) shows a snapshot. In addition to a ring pattern one can observe a slight interference pattern resulting from the wall reflection. We used a 300×150 spatial grid.

Navier-Stokes limits. We study an example for the *incompressible Navier-Stokes* limit. Consider a rectangular vessel with three exits at the left wall. From a larger port A at the top and a smaller port C at the bottom a flow is streaming in with a fixed velocity $\bar{\mathbf{v}}$. At port B adjacent to port A, the fluid is connected to a fluid with constant pressure p_0. Through this port the flow may exit from the vessel. According to [4], the incompressible limit is obtained by taking the limit $\mathrm{Kn} \to 0$ while keeping the ratio $\bar{\mathbf{v}} : \mathrm{Kn}$ (and with this the Stroughal number) constant. Fig. 4 shows the corresponding steady stream lines, one for the Knudsen number $\mathrm{Kn} = 0.056$, the other one for $\mathrm{Kn} = 0.0011$. In the latter case we find a field much smoother and vortices more developed than in the

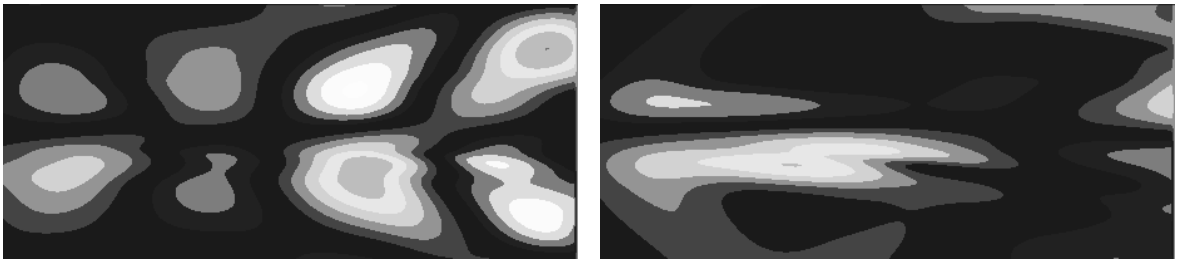

FIGURE 5. (a) Periodic perturbation in uniform flow. (a) Low, (b) high frequency.

first case. In this situation, the maximal density fluctuations are within a range of 0.02% of the mean density. For these calculations, we used a 45×42 spatial grid.

In a second example, we study *mixing properties* of Boltzmann solutions in the Navier-Stokes limit. Introduce a fast periodic source into a uniformly moving flow and let the frequency pass to infinity. The limiting equations will contain the average values of the source but also certain correlations between the involved quantities. We investigate a periodic source within a flow at some uniform velocity. Fig. 5(a) and Fig. 5(b) show the differences between a slow and a faster periodic perturbation. By looking into more detail, one finds some remarkable qualitative differences between these two cases, e.g. the decay of the leading end of the perturbation which is exponential in one case and rational in the other. Such studies are valuable for the understanding of certain phenomena arising at the transition to turbulent flows.

ACKNOWLEDGMENTS

This work was supported by **Deutsche Forschungsgemeinschaft** (DFG), partially in the first priority program "Analysis and Numerics of Conservation Equations".

REFERENCES

1. L. S. Andallah, and H. Babovsky, *Math. Models Methods Appl. Sci.* **13**, 1537–1563 (2003).
2. H. Babovsky, "Hexagonal kinetic models and the numerical simulation of kinetic boundary layers," in *Analysis and Numerics for Conservation Laws*, edited by G. Warnecke, Springer, Berlin, 2005, pp.47–67.
3. H. Babovsky, and L. S. Andallah, "On numerical schemes for a hierarchy of kinetic equations," in *Proceedings ENUMATH05*, Springer, Berlin, 2006, pp.213–220.
4. F. Golse, "The Boltzmann equation and its hydrodynamic limits," in *Evolutionary equations. Vol II*, edited by C.M. Dafermos et al., Elsevier/North Holland, Amsterdam, 2005, pp.159–301.
5. F. Rogier, J. Schneider. A direct method for solving the Boltzmann equation. *Transp. Theory Stat. Phys.*, 23:313–338, 1994.
6. A. Palczewski, J. Schneider and A. V. Bobylev. A consistency result for a discrete velocity model of the Boltzmann equation. *SIAM J. Numer. Anal.*, 34:1865–1883, 1997.
7. L. S. Andallah and H. Babovsky. A discrete Boltzmann equation based on a loosely coupled hexagonal discretization of $\mathbb{R}^2$. *Jahangirnagar University Journal of Sciences*, 28:195–207, 2005.
8. L. S. Andallah. *A hexagonal collision model for the numerical solution of the Boltzmann equation*. PhD thesis, TU Ilmenau, 2004.
9. H. Babovsky, D. Görsch and F. Schilder, "Steady kinetic boundary value problems," in *Lecture Notes on the Discretization of the Boltzmann Equation*, edited by N. Bellomo and R. Gatignol, World Scientific, Singapore, 2002, pp. 131–156.
10. C. Bardos, F. Golse, and D. Levermore, "Macroscopic limits of kinetic equations," in *Multidimensional Hyperbolic Problems and Computations*, edited by J. Glimm and A. J. Majda, Springer, New York, 1991, pp.1–12.